Estimation and Compensation of Frequency Selective TX/RX IQ Imbalance in MIMO OFDM systems

Tim C.W. Schenk, Peter F.M. Smulders and Erik R. Fledderus
Eindhoven University of Technology, Radiocommunication Chair, PO Box 513, 5600 MB Eindhoven, The Netherlands,
Tel. +31 40 247 3436, Fax. +31 40 245 5197, timschenk@ieee.org.

***Abstract*— The influence, digital estimation and compensation of IQ mismatch at both transmitter (TX) and receiver (RX) side of a direct-conversion based multiple antenna OFDM system are presented in this paper. The resulting IQ imbalance can be split into a frequency independent and a frequency selective part. For estimation and compensation a two-step approach is presented, combining a data-aided and decision directed approach. First the frequency independent IQ imbalance is estimated using a preamble and, subsequently, the frequency selective IQ imbalance is removed using adaptive filtering. A numerical performance analysis reveals that the presented approach effectively mitigates the influence of IQ mismatch in OFDM-based space division multiplexing systems experiencing both TX and RX IQ imbalance.**

I. Introduction

The advantages of multiple-input multiple-output orthogonal frequency division multiplexing (MIMO OFDM) as basis for next-generation high data-rate broadband wireless systems, have been reported in many publications over the last few years. Many challenges, however, remain in the efficient and low-cost implementation of these kind of systems, especially since they involve multiple radio front-ends. An obvious solution is the application of *direct-conversion* [1] in both transmitter (TX) and receiver (RX), since it enables monolithic integration of the analogue front-ends.

One of the problems of these homodyne TXs/RXs, however, is that tolerances in the used components for up- and down-conversion can easily result in a phase and/or amplitude imbalance between the in-phase (I) and quadrature phase (Q) signals. Different mismatches can occur in the TX and RX, but regarding their influence they can be divided into two groups: frequency independent (FI) and frequency selective (FS) IQ imbalance. An example of the first group is the mismatch which occurs when the phase shift between the local oscillator signals used for up/down-conversion of the I and Q signal is not exactly 90 degrees. The FS IQ imbalance is mainly caused by mismatch between the filters in the I and Q path, and is dominated by the low-pass filters (LPFs) in the I and Q arms of the RX [2].

The influence and compensation of FI IQ imbalance in direct-conversion based single-input single-output (SISO) OFDM systems has been treated in several publications. Correction techniques for RX-caused IQ imbalance were proposed in e.g. [3]–[5], while a correction approach for TX-caused IQ imbalance was proposed in [6]. The authors of [7] study the combined influence of TX and RX IQ imbalance and propose a compensation approach. Recently, the influence and compensation of IQ imbalance in multiple antenna OFDM systems was addressed in [8]–[10].

The study presented in this paper extends previous work by considering the influence of both TX and RX IQ imbalance in multiple-antenna OFDM systems, where every TX/RX branch will experience a different IQ imbalance. Furthermore, not only compensation of the IQ imbalance is proposed, like in [7]–[9], but also estimation of the imbalance parameters, which enables the possible compensation of IQ mismatch in adaptive RF front-ends. The estimation and compensation approach proposed in this paper consists of two steps. In a first step the FI IQ imbalance is estimated using a preamble and in a second step the FS IQ imbalance is removed using decision directed adaptive filtering.

The outline of the paper is as follows. Section II shows the influence of FI and FS IQ mismatch in MIMO OFDM systems. Two estimation approaches for FI TX and RX IQ imbalance are proposed in Section III. Subsequently, Section IV proposes a compensation approach for FS IQ imbalance. Results from a numerical performance evaluation are presented in Section V. Finally, conclusions are drawn in Section VI.

II. Influence of IQ mismatch

Consider a multiple-antenna based OFDM system with N_t TX and N_r RX branches. The system applies N subcarriers of which $2K$ carriers contain data symbols.

A. Frequency Independent IQ imbalance

The largest part of the IQ imbalance experienced in the TX and RX of a direct-conversion based system will be frequency independent (FI). It occurs, amongst others, in the mixers used for up- and down-conversion to/from radio frequency (RF). For the considered MIMO OFDM system impaired by these imbalances, the received $N_\mathrm{r} \times 1$ signal vector on the kth subcarrier during the mth symbol, $\mathbf{x}_{m,k}$, can be written as

$$\begin{aligned}\mathbf{x}_{m,k} \;=\; &\left(\mathbf{K}_1\mathbf{H}_k\mathbf{G}_1 + \mathbf{K}_2\mathbf{H}^*_{-k}\mathbf{G}_2\right)\mathbf{s}_{m,k} \\ &+ \left(\mathbf{K}_2\mathbf{H}^*_{-k}\mathbf{G}^*_1 + \mathbf{K}_1\mathbf{H}_k\mathbf{G}^*_2\right)\mathbf{s}^*_{m,-k}\;, \qquad (1)\end{aligned}$$

for $k \in \{-K,\ldots,-1,1,\ldots,K\}$, where the asymmetrical modelling of IQ mismatch, as proposed in [11], is applied. Here $\mathbf{H}_k$ denotes the $N_\mathrm{r} \times N_\mathrm{t}$ quasi-static channel transfer matrix for the kth subcarrier and * denotes complex conjugation. The $N_\mathrm{t} \times 1$ transmit symbol vector is denoted by $\mathbf{s}_{m,k}$. Note that here, and throughout the paper, perfect synchronization is assumed.

1-4244-0355-3/06/$20.00 (c) 2006 IEEE

This full text paper was peer reviewed at the direction of IEEE Communications Society subject matter experts for publication in the IEEE ICC 2006 proceedings.

It can be concluded from (1) that the received signal on the kth carrier is a combination of the MIMO signal vectors transmitted on carrier k and on its mirror carrier $-k$. In (1) the TX IQ imbalance is contained in the $N_\mathrm{t} \times N_\mathrm{t}$ matrices $\mathbf{G}_1$ and $\mathbf{G}_2$ and the RX IQ imbalance in the $N_\mathrm{r} \times N_\mathrm{r}$ matrices $\mathbf{K}_1$ and $\mathbf{K}_2$, which are defined as

$$\mathbf{G}_1 = (\mathbf{I} + \boldsymbol{g}_\mathrm{T} e^{j\boldsymbol{\phi}_\mathrm{T}})/2 \ , \qquad \mathbf{G}_2 = \mathbf{I} - \mathbf{G}_1^* \ , \tag{2}$$

$$\mathbf{K}_1 = (\mathbf{I} + \boldsymbol{g}_\mathrm{R} e^{-j\boldsymbol{\phi}_\mathrm{R}})/2 \ , \qquad \mathbf{K}_2 = \mathbf{I} - \mathbf{K}_1^* \ , \tag{3}$$

where $\mathbf{I}$ denotes the identity matrix. The imbalance matrices are defined as

$$\boldsymbol{\phi}_\mathrm{X} = \mathrm{diag}\{\phi_{\mathrm{X},1}, \phi_{\mathrm{X},2}, \ldots, \phi_{\mathrm{X},N_\mathrm{x}}\} \ , \tag{4}$$

$$\boldsymbol{g}_\mathrm{X} = \mathrm{diag}\{g_{\mathrm{X},1}, g_{\mathrm{X},2}, \ldots, g_{\mathrm{X},N_\mathrm{x}}\} \ , \tag{5}$$

where $\mathrm{X} \in \{\mathrm{T}, \mathrm{R}\}$ and $N_\mathrm{x} \in \{N_\mathrm{t}, N_\mathrm{r}\}$. Here $g_{\mathrm{X},n}$ and $\phi_{\mathrm{X},n}$ are the amplitude and phase imbalance for the nth branch, respectively. When there are no imbalances, these parameters are 1 and 0, respectively. Special cases occur when only RX IQ imbalance is present, i.e., $\mathbf{G}_1 = \mathbf{I}$ and $\mathbf{G}_2 = \mathbf{0}$, and when there is only TX IQ imbalance, i.e., $\mathbf{K}_1 = \mathbf{I}$ and $\mathbf{K}_2 = \mathbf{0}$.

B. RX LPF-caused Frequency Selective IQ imbalance

Frequency selective (FS) IQ imbalance occurs due to mismatches between filters and differences in delay in the I and Q branches. Although it also occurs in the TX, it is dominant in the LPFs in the I and Q paths of the RX. That is why the FS IQ imbalance is here modeled as a mismatch between the LPFs in the RX, only. The received signal on the kth subcarrier, only impaired by this LPF mismatch, is then given by

$$\mathbf{x}_{m,k} = \frac{\boldsymbol{\Upsilon}_{\mathrm{I},k} + \boldsymbol{\Upsilon}_{\mathrm{Q},k}}{2} \mathbf{H}_k \mathbf{s}_{m,k} + \frac{\boldsymbol{\Upsilon}_{\mathrm{I},-k} - \boldsymbol{\Upsilon}_{\mathrm{Q},-k}}{2} \mathbf{H}_{-k}^* \mathbf{s}_{m,-k}^*, \tag{6}$$

where the $N_\mathrm{r} \times N_\mathrm{r}$ diagonal matrices $\boldsymbol{\Upsilon}_{\mathrm{I},k}$ and $\boldsymbol{\Upsilon}_{\mathrm{Q},k}$ model the frequency response (of the LPFs) on the kth carrier for the I and Q branches, respectively. It is clear from (6) that when there is no mismatch, i.e., $\boldsymbol{\Upsilon}_{\mathrm{I},k} = \boldsymbol{\Upsilon}_{\mathrm{Q},k}$, there is no leakage of the mirror carrier into the desired signal.

C. FI and FS IQ imbalance

Any practical system, however, would experience a combination of the mismatch effects presented in Section II-A and II-B. The received signal vector on the kth carrier during the mth symbol is then given by

$$\begin{aligned} \mathbf{x}_{m,k} = \ & (\hat{\mathbf{K}}_{1,k} \hat{\mathbf{H}}_k \mathbf{G}_1 + \hat{\mathbf{K}}_{2,-k} \hat{\mathbf{H}}_{-k}^* \mathbf{G}_2) \mathbf{s}_{m,k} \\ & + (\hat{\mathbf{K}}_{2,-k} \hat{\mathbf{H}}_{-k}^* \mathbf{G}_1^* + \hat{\mathbf{K}}_{1,k} \hat{\mathbf{H}}_k \mathbf{G}_2^*) \mathbf{s}_{m,-k}^* \ , \end{aligned} \tag{7}$$

where

$$\hat{\mathbf{K}}_{1,k} = (\mathbf{I} + \boldsymbol{\Upsilon}_{\mathrm{I},k}^{-1} \boldsymbol{\Upsilon}_{\mathrm{Q},k} \boldsymbol{g}_\mathrm{R} e^{-j\boldsymbol{\phi}_\mathrm{R}})/2 \ , \tag{8}$$

$$\hat{\mathbf{K}}_{2,-k} = \mathbf{I} - \hat{\mathbf{K}}_{1,k}^* \ , \tag{9}$$

$$\hat{\mathbf{H}}_k = \boldsymbol{\Upsilon}_{\mathrm{I},k} \mathbf{H}_k \ . \tag{10}$$

Here we used that $\boldsymbol{\Upsilon}_{\mathrm{I},k} = \boldsymbol{\Upsilon}_{\mathrm{I},-k}^*$ and $\boldsymbol{\Upsilon}_{\mathrm{Q},k} = \boldsymbol{\Upsilon}_{\mathrm{Q},-k}^*$, since $\boldsymbol{\Upsilon}_\mathrm{I}$ and $\boldsymbol{\Upsilon}_\mathrm{Q}$ are the frequency responses of real filters.

III. Estimation of Frequency Independent IQ imbalance

This paper proposes the use of a two-step method for estimation and compensation of the IQ imbalance, which enables us to exploit the specific properties of the two kinds of IQ imbalance, discussed above. In the first step, as described in this section, the FI IQ imbalance parameters, i.e., $\boldsymbol{g}_\mathrm{T}$, $\boldsymbol{\phi}_\mathrm{T}$, $\boldsymbol{g}_\mathrm{R}$ and $\boldsymbol{\phi}_\mathrm{R}$, are estimated using a preamble and, subsequently, in a second step, as described in Section IV, an adaptive filtering based algorithm compensates for the FS IQ imbalance. It is noted, however, that the proposed approaches can also be applied separately.

A. Preamble-based estimation

The proposed method for FI IQ imbalance estimation is based on a data-aided approach, where a piece of known data, i.e., preamble, is preceding the data transmission. This preamble is generally used for synchronization and channel estimation, but here we propose to use it as well for the estimation of the imbalance parameters. The estimated parameters can be used to correct for this imbalance in the baseband part of the receiver, but they also could be fed back to the RF front-ends, enabling adjustments there.

Efficient estimation of both the MIMO channel matrix and the IQ matrices (2) and (3) requires certain properties of the preamble. An example of a possible preamble is proposed by the authors in [10]. This preamble is a MIMO extension of the BPSK-based single-antenna preamble in [6]. Basically, the preamble uses Hadamard sequences to achieve orthogonality between subcarriers k and $-k$ and between the different TX branches.

Using this preamble, one finds two transfer matrices, $\mathbf{C}_k^+$ and $\mathbf{C}_k^-$, which are obtained when the signs of the training symbols on carrier k and $-k$ are equal and different, respectively. When it is assumed, for now, that there is only FI IQ imbalance, the obtained transfer matrices are given by

$$\mathbf{C}_k^+ = \mathbf{K}_1 \mathbf{H}_k (\mathbf{G}_1 + \mathbf{G}_2^*) + \mathbf{K}_2 \mathbf{H}_{-k}^* (\mathbf{G}_1^* + \mathbf{G}_2) \ , \tag{11}$$

$$\mathbf{C}_k^- = \mathbf{K}_1 \mathbf{H}_k (\mathbf{G}_1 - \mathbf{G}_2^*) + \mathbf{K}_2 \mathbf{H}_{-k}^* (\mathbf{G}_2 - \mathbf{G}_1^*) \ . \tag{12}$$

From (11) and (12) we can, subsequently, find the channel and FI IQ imbalance parameters using the algorithms presented in Sections III-B and III-C.

B. TX and RX IQ mismatch estimation

Since the MIMO OFDM system experiences both TX and RX IQ imbalance, the estimation problem in (11) and (12) can not be solved directly. Therefore, (11) and (12) are simplified by making the following approximations

$$\mathbf{G}_1 \pm \mathbf{G}_2^* \approx \mathbf{G}_1 \qquad \text{and} \qquad \pm \mathbf{G}_1^* + \mathbf{G}_2 \approx \pm \mathbf{G}_1^* \ , \tag{13}$$

which are valid for small values of TX IQ imbalance. The expressions for the MIMO transfer matrices in (11) and (12) then reduce to

$$\hat{\mathbf{C}}_k^+ = \mathbf{K}_1 \mathbf{H}_k \mathbf{G}_1 + \mathbf{K}_2 \mathbf{H}_{-k}^* \mathbf{G}_1^* \ , \tag{14}$$

$$\hat{\mathbf{C}}_k^- = \mathbf{K}_1 \mathbf{H}_k \mathbf{G}_1 - \mathbf{K}_2 \mathbf{H}_{-k}^* \mathbf{G}_1^* \ . \tag{15}$$

Applying these approximated expressions, the RX imbalance parameters can be estimated. Hereto we define

$$\hat{\mathbf{C}}_{k,\mathrm{s}} = (\hat{\mathbf{C}}_k^+ + \hat{\mathbf{C}}_k^-)/2 = \mathbf{K}_1\mathbf{H}_k\mathbf{G}_1 \ , \quad (16)$$

$$\hat{\mathbf{C}}_{k,\mathrm{d}} = (\hat{\mathbf{C}}_k^+ - \hat{\mathbf{C}}_k^-)/2 = \mathbf{K}_2\mathbf{H}_{-k}^*\mathbf{G}_1^* \ . \quad (17)$$

Subsequently, we find for the kth subcarrier

$$\begin{aligned}\mathbf{Q}_k &= (\hat{\mathbf{C}}_{k,\mathrm{s}} - \hat{\mathbf{C}}_{-k,\mathrm{d}}^*)(\hat{\mathbf{C}}_{k,\mathrm{s}} + \hat{\mathbf{C}}_{-k,\mathrm{d}}^*)^\dagger \\ &= \boldsymbol{g}_\mathrm{R}\exp(-j\boldsymbol{\phi}_\mathrm{R}) \ , \end{aligned} \quad (18)$$

where † denotes the pseudo-inverse. The estimates of the RX phase and amplitude imbalance matrices are then easily found from (18) as

$$\tilde{\boldsymbol{\phi}}_{\mathrm{R},k} = -\arctan\left(\mathcal{I}\{\mathbf{Q}_k\}\mathcal{R}\{\mathbf{Q}_k\}^{-1}\right) \ , \quad (19)$$

$$\tilde{\boldsymbol{g}}_{\mathrm{R},k} = \sqrt{\mathcal{R}\{\mathbf{Q}_k\}^2 + \mathcal{I}\{\mathbf{Q}_k\}^2} \ , \quad (20)$$

respectively. Here $\tilde{\alpha}$ indicates the estimate of parameter α and $\mathcal{R}\{\cdot\}$ and $\mathcal{I}\{\cdot\}$ give the real and imaginary part of their arguments.

Improved estimates of these RX imbalance parameters are obtained by averaging over the frequency index k, which exploits the frequency independence of the IQ imbalance. A further improvement is achieved by making use of the fact that the IQ parameters are time-invariant. This can be done by averaging the imbalance parameters with those found in the previous P packets. This averaging over time and frequency yields the improved estimates $\bar{\boldsymbol{g}}_\mathrm{R}$ and $\bar{\boldsymbol{\phi}}_\mathrm{R}$.

Following this, we can go back to the original expressions in (11) and (12). Using these expressions and the estimated RX IQ imbalance parameters, the estimate of the MIMO channel matrix for the kth carrier is found by

$$\tilde{\mathbf{H}}_k = (\bar{\mathbf{Q}} + \bar{\mathbf{Q}}^*)^{-1}(\bar{\mathbf{Q}}^*(\mathbf{C}_k^+ + \mathbf{C}_{-k}^{+\,*}) + \mathbf{C}_k^+ - \mathbf{C}_{-k}^{+\,*}), \quad (21)$$

where $\bar{\mathbf{Q}} = \bar{\boldsymbol{g}}_\mathrm{R}\exp(-j\bar{\boldsymbol{\phi}}_\mathrm{R})$.

Finally, to estimate the TX IQ imbalance parameters, we rewrite (12) for carrier k and its mirror $-k$ in matrix notation as

$$\begin{bmatrix} \mathbf{C}_k^- \\ \mathbf{C}_{-k}^- \end{bmatrix} = \underbrace{\begin{bmatrix} \mathbf{K}_1\mathbf{H}_k & \mathbf{K}_2\mathbf{H}_{-k}^* \\ \mathbf{K}_1\mathbf{H}_{-k} & \mathbf{K}_2\mathbf{H}_k^* \end{bmatrix}}_{\mathbf{T}_k} \begin{bmatrix} \mathbf{g}_\mathrm{T}e^{j\boldsymbol{\phi}_\mathrm{T}} \\ -\mathbf{g}_\mathrm{T}e^{-j\boldsymbol{\phi}_\mathrm{T}} \end{bmatrix} . \quad (22)$$

From (22) it is then easily found that

$$\begin{bmatrix} \mathbf{M}_{1,k} \\ \mathbf{M}_{2,k} \end{bmatrix} = \begin{bmatrix} \tilde{\mathbf{g}}_\mathrm{T}e^{j\tilde{\boldsymbol{\phi}}_\mathrm{T}} \\ -\tilde{\mathbf{g}}_\mathrm{T}e^{-j\tilde{\boldsymbol{\phi}}_\mathrm{T}} \end{bmatrix} = \tilde{\mathbf{T}}_k^\dagger \begin{bmatrix} \mathbf{C}_k^- \\ \mathbf{C}_{-k}^- \end{bmatrix} \ , \quad (23)$$

where $\tilde{\mathbf{T}}_k$ is constructed from the estimated channel and RX IQ parameters, derived in the previous steps. From (23) the TX IQ imbalance parameters for the kth subcarrier are estimated as

$$\tilde{\boldsymbol{\phi}}_{\mathrm{T},k} = \arctan\Big(\mathcal{I}\{\mathbf{M}_{1,k} - \mathbf{M}_{2,k}^*\}\mathcal{R}\{\mathbf{M}_{1,k} - \mathbf{M}_{2,k}^*\}^{-1}\Big) , \quad (24)$$

$$\tilde{\boldsymbol{g}}_{\mathrm{T},k} = \frac{\sqrt{\mathcal{R}\{\mathbf{M}_{1,k} - \mathbf{M}_{2,k}^*\}^2 + \mathcal{I}\{\mathbf{M}_{1,k} - \mathbf{M}_{2,k}^*\}^2}}{2} \ . \quad (25)$$

Again, the improved estimates of the imbalance parameters, i.e., $\bar{\boldsymbol{\phi}}_\mathrm{T}$ and $\bar{\boldsymbol{g}}_\mathrm{T}$, are found by averaging the imbalance estimates over the subcarriers and the previous P packets.

The estimates of the FI TX and RX IQ imbalance parameters can be used to correct for the IQ imbalance. The estimate of the MIMO channel matrix can, subsequently, be used to retrieve the transmitted symbols from the IQ imbalance corrected signals.

C. Improved estimation

The data-aided approach proposed in Section III-B is based on the assumption that the TX IQ imbalance is relatively small, which limits the performance in estimation of the TX/RX imbalance and channel parameters. Although this can be partly overcome by averaging over the different subcarriers and packets, the approximations of (13) create a bias in the estimates, which increases with increasing TX imbalance.

Therefore, this section proposes an improved technique, which applies the algorithm of Section III-B only for the first received packet. For all other packets the estimates of $\boldsymbol{g}_\mathrm{T}$, $\boldsymbol{\phi}_\mathrm{T}$, $\boldsymbol{g}_\mathrm{R}$ and $\boldsymbol{\phi}_\mathrm{R}$ from the preceding packet are used to solve the estimation problem. Note that these parameters are system parameters and can thus, in contrast to the wireless channel $\mathbf{H}$, be assumed to be constant over a large number of packets.

For an improved estimate of the MIMO channel matrix for the kth carrier during the $(p+1)$th packet transmission (for $p \geq 1$), we can then exploit (11) and (12) on carrier k and $-k$:

$$\begin{aligned}&\tilde{\mathbf{H}}_k(p+1) = \\ &\Big[\tilde{\boldsymbol{\alpha}}^\dagger(p)\{\mathbf{B}_2(p+1)\tilde{\boldsymbol{\beta}}^*(p) + \mathbf{B}_3(p+1)\}\{\tilde{\boldsymbol{\beta}}(p) + \tilde{\boldsymbol{\beta}}^*(p)\}^\dagger \\ &+\{\tilde{\boldsymbol{\alpha}}(p) + \tilde{\boldsymbol{\alpha}}^*(p)\}^\dagger\{\tilde{\boldsymbol{\alpha}}^*(p)\mathbf{B}_1(p+1) + \mathbf{B}_2(p+1)\}\Big]/2 \ , \end{aligned} \quad (26)$$

where (p) denotes the packet index and where we defined

$$\mathbf{B}_1 = \mathbf{C}_k^+ + \mathbf{C}_{-k}^{+\,*} = \mathbf{H}_k + \mathbf{H}_{-k}^* \ , \quad (27)$$

$$\mathbf{B}_2 = \mathbf{C}_k^+ - \mathbf{C}_{-k}^{+\,*} = \boldsymbol{\alpha}\mathbf{H}_k - \boldsymbol{\alpha}^*\mathbf{H}_{-k}^* \ , \quad (28)$$

$$\mathbf{B}_3 = \mathbf{C}_k^- + \mathbf{C}_{-k}^{-\,*} = \boldsymbol{\alpha}\mathbf{H}_k\boldsymbol{\beta} + \boldsymbol{\alpha}^*\mathbf{H}_{-k}^*\boldsymbol{\beta}^* \ , \quad (29)$$

$$\boldsymbol{\alpha} = \boldsymbol{g}_\mathrm{R}e^{-j\boldsymbol{\phi}_\mathrm{R}} \ , \quad (30)$$

$$\boldsymbol{\beta} = \boldsymbol{g}_\mathrm{T}e^{j\boldsymbol{\phi}_\mathrm{T}} \ . \quad (31)$$

Subsequently, estimates of the TX IQ imbalance parameters can be found using (24) and (25), where we use the MIMO channel estimate found in (26) and the RX IQ imbalance estimated during the pth packet to construct $\tilde{\mathbf{T}}_k(p+1)$. The new estimates of the TX IQ parameters, after averaging over the subcarriers, are then used to construct $\tilde{\boldsymbol{\beta}}(p+1)$.

Following that, the improved estimates of the RX IQ imbalance parameters on the kth carrier are found by

$$[\tilde{\mathbf{K}}_{1,k}(p+1) \ \ \tilde{\mathbf{K}}_{2,k}(p+1)] = \mathbf{C}_k(p+1)\mathbf{Y}_k^\dagger(p+1) \ , \quad (32)$$

where we defined

$$\mathbf{C}_k(p) = \begin{bmatrix} \mathbf{C}_k^+(p) & \mathbf{C}_k^-(p) & \mathbf{C}_{-k}^+(p) & \mathbf{C}_{-k}^-(p) \end{bmatrix} \ , \quad (33)$$

$$\mathbf{Y}_k(p) = \begin{bmatrix} \tilde{\mathbf{H}}_k(p) & \tilde{\mathbf{H}}_k(p)\tilde{\boldsymbol{\beta}}(p) & \tilde{\mathbf{H}}_{-k}(p) & \tilde{\mathbf{H}}_{-k}(p)\tilde{\boldsymbol{\beta}}(p) \\ \tilde{\mathbf{H}}_{-k}^*(p) & -\tilde{\mathbf{H}}_{-k}^*(p)\tilde{\boldsymbol{\beta}}^*(p) & \tilde{\mathbf{H}}_k^*(p) & -\tilde{\mathbf{H}}_k^*(p)\tilde{\boldsymbol{\beta}}^*(p) \end{bmatrix} . \quad (34)$$

From (32) we construct

$$\tilde{\boldsymbol{\alpha}}_k(p+1) = \tilde{\mathbf{K}}_{1,k}(p+1) - \tilde{\mathbf{K}}^*_{2,k}(p+1) \ , \qquad (35)$$

which is used to find the imbalance matrices

$$\tilde{\phi}_{\mathrm{R},k} \ = \ -\arctan\left(\mathcal{I}\{\tilde{\boldsymbol{\alpha}}_k(p+1)\}\mathcal{R}\{\tilde{\boldsymbol{\alpha}}_k(p+1)\}^{-1}\right) , \qquad (36)$$

$$\tilde{\boldsymbol{g}}_{\mathrm{R},k} \ = \ \sqrt{\mathcal{R}\{\tilde{\boldsymbol{\alpha}}_k(p+1)\}^2 + \mathcal{I}\{\tilde{\boldsymbol{\alpha}}_k(p+1)\}^2} \ . \qquad (37)$$

Finally, averaging these estimates over the different subcarriers provides all estimates for the $(p+1)$th packet.

To reduce the influence of noise on the error in estimation of the IQ imbalance parameters, averaging over different packets as in Section III-B can be applied. This is, however, only beneficial when the errors in the estimates for the pth packet do not dominate the errors in estimates for the $(p+1)$th packet. From simulations this was found to be valid for $p > 10$.

IV. Compensation of Frequency selective IQ mismatch

Data-aided estimation of the FS IQ imbalance parameters would require a large amount of pilot data and thus impose a large overhead. Therefore, this section proposes a decision directed approach. The IQ imbalance parameters are not explicitly estimated, but an adaptive filter matrix is applied, one for every subcarrier pair, to retrieve the transmitted data. The filter weights are adapted such that the filter compensates for the combined influence of the MIMO channel matrix and the FI and FS IQ imbalance.

For this purpose the expression for the received signal on the kth carrier in this case of both FI and FS IQ imbalance, (7), is rewritten to

$$\underbrace{\begin{bmatrix} \mathbf{x}_{m,k} \\ \mathbf{x}^*_{m,-k} \end{bmatrix}}_{\hat{\mathbf{x}}_{m,k}} = \begin{bmatrix} \mathbf{A}_k & \mathbf{B}_k \\ \mathbf{B}^*_{-k} & \mathbf{A}^*_{-k} \end{bmatrix} \underbrace{\begin{bmatrix} \mathbf{s}_{m,k} \\ \mathbf{s}^*_{m,-k} \end{bmatrix}}_{\hat{\mathbf{s}}_{m,k}} , \qquad (38)$$

where

$$\mathbf{A}_k \ = \ \hat{\mathbf{K}}_{1,k}\hat{\mathbf{H}}_k\mathbf{G}_1 + \hat{\mathbf{K}}_{2,-k}\hat{\mathbf{H}}^*_{-k}\mathbf{G}_2 \ , \qquad (39)$$

$$\mathbf{B}_k \ = \ \hat{\mathbf{K}}_{2,-k}\hat{\mathbf{H}}^*_{-k}\mathbf{G}^*_1 + \hat{\mathbf{K}}_{1,k}\hat{\mathbf{H}}_k\mathbf{G}^*_2 \ . \qquad (40)$$

The data can now be recovered by applying the $2N_{\mathrm{t}} \times 2N_{\mathrm{r}}$ filter matrix $\mathbf{W}_{m,k}$ to the received data vector, yielding the estimates of the transmitted symbols

$$\begin{bmatrix} \tilde{\mathbf{s}}_{m,k} \\ \tilde{\mathbf{s}}^*_{m,-k} \end{bmatrix} = \mathbf{W}_{m,k} \begin{bmatrix} \mathbf{x}_{m,k} \\ \mathbf{x}^*_{m,-k} \end{bmatrix} \ . \qquad (41)$$

For the adaptation of the filter matrix $\mathbf{W}_{m,k}$ the exponentially weighted recursive least-squares (RLS) algorithm [12] was chosen. The initial filter matrix $\mathbf{W}_{0,k}$ is found by using the estimates of the FI IQ imbalance and MIMO channel matrices from the data-aided estimation of Section III. The resulting filter matrix is given by

$$\mathbf{W}_{0,k} = \begin{bmatrix} \mathbf{A}_k & \mathbf{B}_k \\ \mathbf{B}^*_{-k} & \mathbf{A}^*_{-k} \end{bmatrix}^{\dagger} \ . \qquad (42)$$

The adaptation process can be summarized as follows [12]:

$$\mathbf{P}_{0,k} = \delta^{-1}\mathbf{I}$$

For the symbols $m = 1, 2, \ldots, M$

$$\begin{aligned} \boldsymbol{\Pi}_{m,k} &= \mathbf{P}_{m-1,k}\hat{\mathbf{x}}_{m,k} \\ \boldsymbol{k}_{m,k} &= \boldsymbol{\Pi}_{m,k}(\lambda + \hat{\mathbf{x}}^H_{m,k}\boldsymbol{\Pi}_{m,k})^{-1} \\ \mathbf{e}_{m,k} &= \mathcal{D}\{\mathbf{W}_{m-1,k}\hat{\mathbf{x}}_{m,k}\} - \mathbf{W}_{m-1,k}\hat{\mathbf{x}}_{m,k} \\ \mathbf{W}^H_{m,k} &= \mathbf{W}^H_{m-1,k} + \boldsymbol{k}_{m,k}\mathbf{e}^H_{m,k} \\ \mathbf{P}_{m,k} &= \lambda^{-1}\mathbf{P}_{m-1,k} - \lambda^{-1}\boldsymbol{k}_{m,k}\hat{\mathbf{x}}^H_{m,k}\mathbf{P}_{m-1,k} \ , \end{aligned}$$

where $\mathcal{D}\{\cdot\}$ gives the hard decision based slicing estimate of its input. The regularization parameter δ has to be chosen inversely proportional to the signal-to-noise ratio (SNR) and the exponential weighting factor λ is chosen to be smaller than 1.

V. Performance Evaluation

To evaluate the performance of the estimation and compensation techniques proposed in the previous sections, Monte Carlo simulations were performed. As a test-case a 2×2 MIMO extension of the IEEE 802.11a standard [13] was chosen. For this system the number of subcarriers N = 64, of which $2K$ = 48 carry data. The Hadamard-based preamble as proposed in [10] was used for channel estimation and in systems experiencing IQ imbalance it was used for both channel and IQ imbalance parameter estimation.

First the data-aided estimation of the FI IQ imbalance parameters, as proposed in Section III, was tested. Figure 1 reports the mean-squared-error (MSE) in the estimation of the diagonal elements of $\mathbf{K}_1$ (in solid lines) and $\mathbf{G}_1$ (in dashed lines) and the elements of the MIMO channel matrix $\mathbf{H}$ (in dotted lines) as function of the SNR per RX branch. In the simulations a spatial uncorrelated Rayleigh faded channel was applied. The power-delay-profile was exponential decaying and the rms delay spread was equal to 100 ns. The channel is modeled as quasi-static, i.e., the channel is constant over the length of the packet, but generated independently for the different packets. The imbalance parameters were chosen as $\mathbf{g}_{\mathrm{T}} = \mathbf{g}_{\mathrm{R}} = \mathrm{diag}\{1.1, 1.1\}$ and $\boldsymbol{\phi}_{\mathrm{T}} = \boldsymbol{\phi}_{\mathrm{R}} = \mathrm{diag}\{3^\circ, 3^\circ\}$, which corresponds to a case with severe IQ imbalance. The results are given for the first packet (*original*) and for both the method of Section III-B (*averaging*) and Section III-C (*improved*) after $P = 20$ packets.

It can be concluded from Fig. 1 that the MSE curve for the estimates of $\mathbf{K}_1$ and $\mathbf{H}$ after the first packet show flooring, which is improved by the method of Section III-B by averaging over 20 packets. Note that only the IQ imbalance parameters are averaged, *not* the channel estimates. The flooring at high SNR, however, remains. In contrast, the method of Section III-C does solve the flooring at high SNR, i.e., the MSE of $\mathbf{K}_1$ and $\mathbf{H}$ fall of linearly with SNR here. At low SNR, however, a small increase in MSE of $\mathbf{K}_1$ occurs, compared to the averaging method. The MSE in estimation of $\mathbf{G}_1$ gains less from the averaging algorithm, which can be attributed to a bias in the estimation.

Results from bit-error-rate (BER) simulations are presented in Fig. 2 for a 2×2 space division multiplexing system [14] applying Zero-Forcing (ZF) based MIMO detection. The

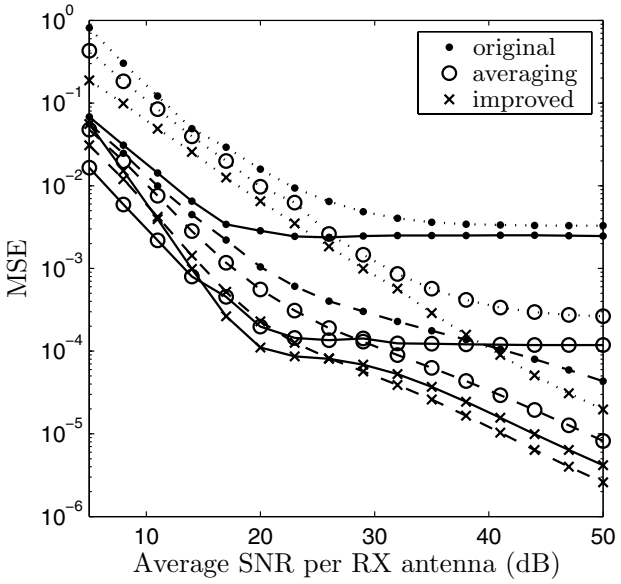

Fig. 1. MSE in estimation of the imbalance parameters $\mathbf{K}_1$ (—), $\mathbf{G}_1$ (−−) and $\mathbf{H}$ ($\cdots$). $\mathbf{g}_R = \mathbf{g}_T = \text{diag}\{1.1, 1.1\}$ and $\boldsymbol{\phi}_T = \boldsymbol{\phi}_R = \{3°, 3°\}$. Results are given for the first packet (*original*) and for P = 20 packets (*averaging* and *improved*).

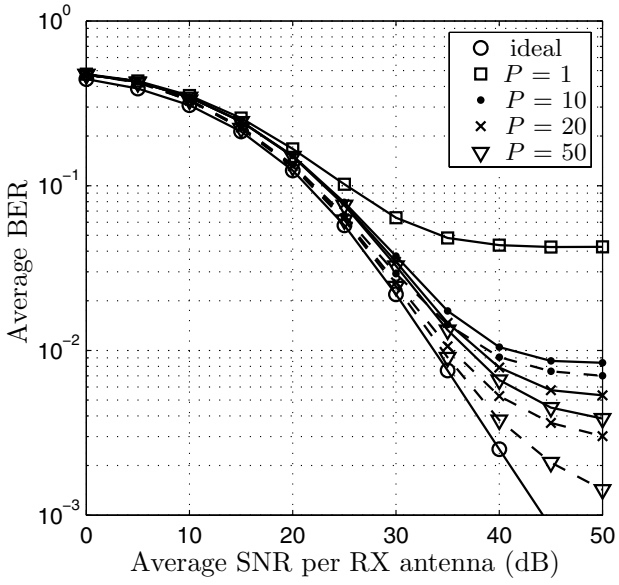

Fig. 2. BER performance of a 2×2 system applying ZF detection, 64-QAM modulation and no coding. The IQ imbalance parameters were $\mathbf{g}_R = \mathbf{g}_T = \text{diag}\{1.1, 1.1\}$ and $\boldsymbol{\phi}_T = \boldsymbol{\phi}_R = \{3°, 3°\}$. Results are given for the averaging (—) and improved (−−) method for $P \in \{1, 10, 20, 50\}$.

correction of the IQ imbalance applies the estimates from the algorithms in Section III. The channel and IQ imbalance parameters were equal to those of the simulations of Fig. 1. The BER results are given for different number of packets P. As a reference the BER of a system not experiencing IQ imbalance (*ideal*), but applying channel estimation with the same preamble, is given.

It is clear from Fig. 2 that the BER improves with increasing P for both methods. The improvements in BER performance are, however, higher for the method proposed in Section III-C. For this method the degradation compared to the *ideal* BER is smaller and lower BER flooring occurs than for the method of Section III-B. When we combine these results with the MSE results, we can conclude that the improvement in BER performance achieved by the approach of Section III-C can be mainly attributed to the improved estimates of $\mathbf{K}_1$ and $\mathbf{H}$.

Subsequently, the performance of the combination of estimation and compensation approaches of Section III and IV was tested. Again a 2×2 MIMO system applying 64-QAM modulation was simulated. Now, however, a non-fading perfect orthogonal MIMO channel (AWGN) was applied.

Figure 3 shows results for a system only experiencing FI IQ imbalance (in solid lines) and a system experiencing both FI and FS IQ imbalance (in dashed lines). The FI IQ imbalance parameters were equal to those in the simulations reported above. The FS IQ imbalance was modeled in a similar way as in [7]. The LPFs in the I paths were modeled using a 6th order Chebyshev Type 1 filter with a ripple of 1 dB and a pass band of 0.9 times the sample frequency. The parameters of the LPFs in the Q paths were slightly different, to create the mismatch. The ripple was set to 1.05 dB and the pass band to 0.905 times the sample frequency. The exponential weighting factor λ of the RLS filter was chosen to be 0.99 for the results presented in this paper. The filter was initialized with the estimated from the improved FI IQ imbalance estimation technique of Section III-C, acquired after P=50 packets.

The results in Fig. 3 show that compensation with the estimates from the improved approach of Section III-C (*IQ imb., init. comp.*) does increase the performance of the system, compared to the case with IQ imbalance and no compensation (*IQ imb., no comp.*). However, a performance degradation compared to the reference curve for a system not experiencing IQ imbalance (*no IQ imb.*) still exists. When the adaptive filtering is applied (*IQ imb., AF*), the BER performance improves beyond the curve without IQ imbalance. This can be explained by the fact that the adaptive filtering also improves the estimates of the MIMO channel matrices. This is illustrated by the results for a system that does not experience IQ imbalance, but does apply the AF of Section IV (*no IQ imb., AF*). For the system experiencing both types of IQ imbalance, the performance is slightly worse than that of a system only experiencing FI IQ imbalance.

The convergence of the adaptive filter is tested in simulations where the packetlength was varied. Results of these simulations are depicted in Fig. 4. The same channel, imbalance and filter parameters were used as for the simulations of Fig. 3. The curves for a system not applying compensation (*no comp.*) and for a system not applying the adaptive filtering (*init. comp.*), i.e., a system which only corrects for the FI IQ imbalance estimated in the preamble phase, are given in the figure as reference.

It can be concluded from the results in Fig. 4 that for a packetlength of 5 symbols the gain compared to the initial correction is small. When the packetlength is increased, however, the performance improves largely compared to the system only applying correction based on the initial estimates.

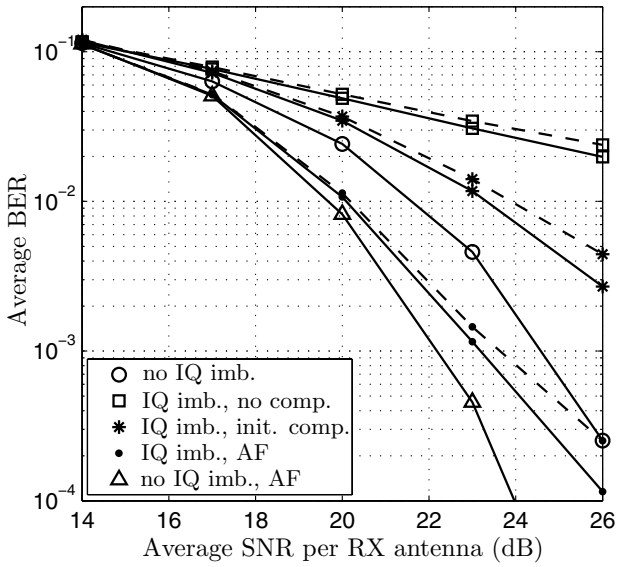

Fig. 3. BER performance of a 2×2 system applying ZF detection, 64-QAM modulation and no coding. $\mathbf{g}_{\mathrm{T}} = \mathbf{g}_{\mathrm{R}} = \mathrm{diag}\{1.1, 1.1\}$, $\boldsymbol{\phi}_{\mathrm{T}} = \boldsymbol{\phi}_{\mathrm{R}} = \mathrm{diag}\{3^\circ, 3^\circ\}$, packetlength is 500 symbols and AF initialization based on P = 50 packets. Results for a system experiencing FI IQ imbalance (—) and for a system experiencing both FI and FS IQ imbalance (− −).

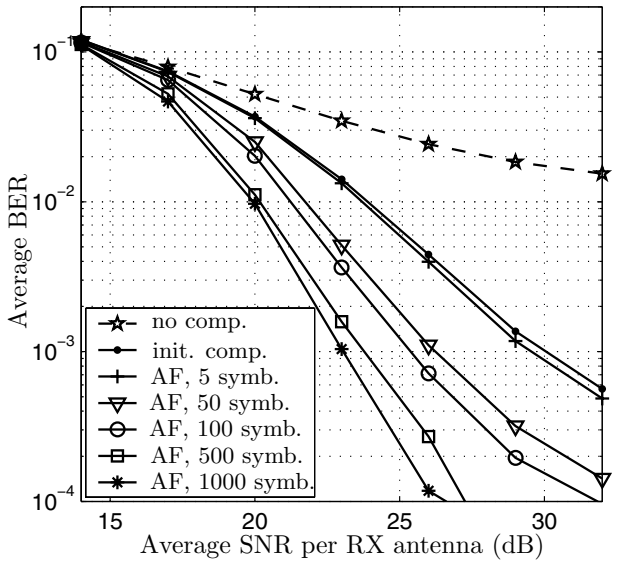

Fig. 4. BER performance of a 2×2 system applying ZF detection, 64-QAM modulation and no coding. $\mathbf{g}_{\mathrm{T}} = \mathbf{g}_{\mathrm{R}} = \mathrm{diag}\{1.1, 1.1\}$, $\boldsymbol{\phi}_{\mathrm{T}} = \boldsymbol{\phi}_{\mathrm{R}} = \mathrm{diag}\{3^\circ, 3^\circ\}$ and filter imbalance. Results for different packetlengths, AF initialization based on P = 50 packets.

It is noted that, when the AF is applied, the first data symbols of the packet are detected with a higher BER than those located further in the packet, since the AF needs several symbols to converge. The reliability of detection of the first symbols can be increased by redetecting the first few symbols, when the the filter weights are converged. This, however, comes at the cost of additional complexity.

VI. Conclusions

The influence of transmitter- and receiver-caused frequency independent and frequency selective IQ mismatch in a multiple-antenna OFDM system has been studied in this paper. A two-step approach for the estimation and compensation of IQ imbalance has been proposed, the steps of which can also be applied separately. In the first step the frequency flat transmitter and receiver IQ imbalance are estimated using a preamble. The estimation approach exploits that the IQ imbalance is time-invariant. Moreover, an improved method is proposed, which exploits the IQ imbalance estimates from previous packets. In the second step data is detected using an adaptive MIMO filter. The initial weights of this filter are determined from the estimates for the FI IQ imbalance and the MIMO channel matrix. In the following steps the adaptive filter also removes the frequency selective part of IQ imbalance using a decision directed approach. From a numerical study it is concluded that the proposed combined estimation and compensation approach provides a considerable improvement in bit-error-rate performance compared to a system applying no compensation for the influence of IQ mismatch.

Although the compensation techniques are proposed for MIMO systems in this paper, they are also well applicable for single-antenna OFDM systems.

References

[1] A.A. Abidi, "Direct-conversion radio transceivers for digital communications," *IEEE J. Solid-State Circuits*, vol. 30, pp. 1399–1410, Dec. 1995.

[2] P. Kiss and V. Prodanov, "One-tap wideband I/Q compensation for zero-IF filters," *IEEE Trans. on Circuits and Systems - I: Regular Papers*, vol. 51, no. 6, pp. 1062–1074, June 2004.

[3] A. Schuchert, R. Hasholzner, and P. Antoine, "A novel IQ imbalance compensation scheme for the reception of OFDM signals," *IEEE Trans. Consumer Electron.*, vol. 47, no. 3, pp. 313–318, Aug. 2001.

[4] J. Tubbax, B. Côme, L. van der Perre, L. Deneire, S. Donnay, and M. Engels, "Compensation of IQ imbalance in OFDM systems," in *Proc. IEEE International Conference on Communications 2003*, May 2003, vol. 5, pp. 3403–3407.

[5] M. Windisch and G. Fettweis, "Standard-independent I/Q imbalance compensation in OFDM direct-conversion receivers," in *Proc. 9th International OFDM Workshop*, Sept. 2004, pp. 57–61.

[6] L. Brötje, S. Vogeler, K.-D. Kammeyer, R. Rueckriem, and S. Fechtel, "Estimation and correction of transmitter-caused I/Q imbalance in OFDM systems," in *Proc. 7th International OFDM Workshop*, Sept. 2002, pp. 178–182.

[7] E. Tsui and J. Lin, "Adaptive IQ imbalance correction for OFDM systems with frequency and timing offsets," in *Proc. IEEE Global Telecommunications Conference*, 2004, pp. 4004–4010.

[8] R.M. Rao and B. Daneshrad, "I/Q mismatch cancellation for MIMO-OFDM systems," in *Proc. IEEE Int. Symp. Pers., Indoor, Mobile Radio Commun. (PIMRC)*, Sept. 2004, vol. 5, pp. 2710–2714.

[9] A. Tarighat and A.H. Sayed, "MIMO OFDM receivers for systems with IQ imbalances," *IEEE Transactions on Signal Processing*, vol. 53, no. 9, pp. 3583–3596, Sept. 2005.

[10] T.C.W. Schenk, P.F.M. Smulders, and E.R. Fledderus, "Estimation and compensation of TX and RX IQ imbalance in OFDM based MIMO systems," in *Proc. IEEE Radio and Wireless Symposium (RWS 2006)*, Jan. 2006, pp. 215–218.

[11] M. Valkama, M. Renfors, and V. Koivunen, "Advanced methods for I/Q imbalance compensation in communication receivers," *IEEE Trans. on Signal Proc.*, vol. 49, pp. 2335–2344, Oct. 2001.

[12] S. Haykin, *Adaptive Filter Theory*, Prentice-Hall, fourth edition, 2002.

[13] *IEEE 802.11a standard*, ISO/IEC 802-11:1999/Amd 1:2000(E).

[14] A. van Zelst, R.D.J. van Nee, and G.A. Awater, "Space division multiplexing (SDM) for OFDM systems," in *Proc. IEEE Vehicular Technology Conf. 2000-Spring*, May 2000, pp. 1070–1074.